ELSEVIER

Materials Science and Engineering B71 (2000) 51–55

MATERIALS SCIENCE & ENGINEERING B

www.elsevier.com/locate/mseb

Spatially resolved defect diagnostics in multicrystalline silicon for solar cells

I. Tarasov [a], S. Ostapenko [a,*], C. Haessler [b], E.-U. Reisner [b]

[a] *University of South Florida, Center for Microelectronics Research, 4202 E Fowler Ave., Tampa, FL 33620, USA*
[b] *BAYER AG, 47812 Krefeld, Germany*

Abstract

Scanning room temperature photoluminescence (PL) spectroscopy was applied to cast multicrystalline Si to assess the electronic properties of high-quality solar-grade material. The intensity of band-to-band emission with the maximum at 1.09 eV positively correlates with minority carrier lifetime measured concurrently using the laser-microwave reflection technique. A point-by-point mapping revealed the linear dependence of the band-to-band PL intensity and lifetime across entire multicrystalline-Si wafers. We have also found at room temperature an intense 'defect' PL band with the maximum at about 0.8 eV in wafer regions with a low band-to-band emission and degraded lifetime. The PL mapping of the 0.8 eV band intensity revealed a linkage to areas of a high dislocation density. Dislocation topography was obtained independently using light scattering technique and mapping the dislocation D-lines at 77 K. PL spectroscopy down to 4.2 K was performed at areas with high and low 'defect' band intensity. The origin of the 0.8 eV band is discussed in a connection with dislocations in multicrystalline Si. We demonstrate advantages of scanning room temperature PL spectroscopy for in-line diagnostics of Si-based materials. © 2000 Elsevier Science S.A. All rights reserved.

Keywords: Photoluminescence; Dislocation; Silicon; Oxygen; Lifetime; Grain boundaries

1. Introduction

The actual strong growth in the photovoltaic market is mainly based on crystalline silicon wafer technology. Specifically multicrystalline silicon (mc-Si) is able to meet both the requirements of a cost-effective large-scale production technique and high solar cell efficiencies. Continuously improving crystallization conditions and solar cell processing sequences have lead to steadily increasing photovoltaic efficiencies of mc-Si solar cells. Based on Baysix® mc-Si, efficiencies between 16 and 17% have been realized with cell processes that seem to be transferable into industrial production. One of the main limiting factors of mc-Si solar cell efficiencies, however, are so-called 'bad regions' with enhanced recombination activity. A further substantial improvement of the efficiencies attainable with mc-Si solar cells can therefore be achieved by reducing and potentially eliminating 'bad regions'. Development of reliable diagnostics of mc-Si performed after various solar cell processing steps is valuable for assessing electronic quality upgrading. In this paper, we report application of scanning room-temperature photoluminescence (PL) spectroscopy in solar grade mc-Si. A correlation of PL mapping performed at two luminescent bands with minority carrier lifetime and distribution of dislocation density allowed suggesting a model of recombination defects located in regions with high recombination activity.

2. Experimental

Multicrystalline silicon 10×10 cm bare wafers were grown using block-casting technique for Baysix® mc-Si. Samples for scanning PL study were quarters of the full size mc-Si wafers.

The PL spectrum was analyzed using a SPEX-500 M grating spectrometer coupled to a liquid nitrogen cooled Ge detector. The 800 nm AlGaAs laser diode

* Corresponding author: Tel.: +1-813-974-2031; fax: +1-813-974-3610.
E-mail address: ostapenk@eng.usf.edu (S. Ostapenko)

PII: S0921-5107(99)00348-7

(10 nm bandwidth) operating in a pulse mode with peak power up to 300 mW was used as the excitation source. The absorption coefficient of the AlGaAs laser in silicon is 12 μm^{-1}, which allowed us to reduce the influence of surface recombination on bulk PL intensity. PL mapping was performed by placing mc-Si wafers on an $X-Z$ moving stage with a spatial resolution controlled by the diameter of the laser spot, which ranged from 0.25 to 3 mm. The PL spectra were corrected to the spectral response of the optical system. Concurrently, a commercial PL mapping system was utilized in this study (http://www.ust1.com). The mapping of effective minority carrier lifetime was performed using a laser-microwave reflection technique with the spatial resolution identical to the PL mapping. Notice that both methods realize a high injection limit for the minority carriers in p-type Si.

Experimentally, structural crystal defects like dislocations are accessible by counting μm-size etch pits after appropriate chemical etching steps (e.g. Secco etchant). This technique, however, is limited to very small areas ($\ll 1$ mm^2). Consequently, for an adjustment of the physical data set employed for simulating the generation of dislocations in mc-Si there is tremendous need for statistically relevant experimental data, i.e. dislocation density distributions over several cm^2 in different parts of the mc-Si ingot. We used a measurement system capable of etch pit density (EPD) mappings over large areas up to 10 × 10 cm wafers. Basically, the EPD system consists of a microscope with computer-controlled automatic focusing, an $x-y$ table, and an image analysis software program.

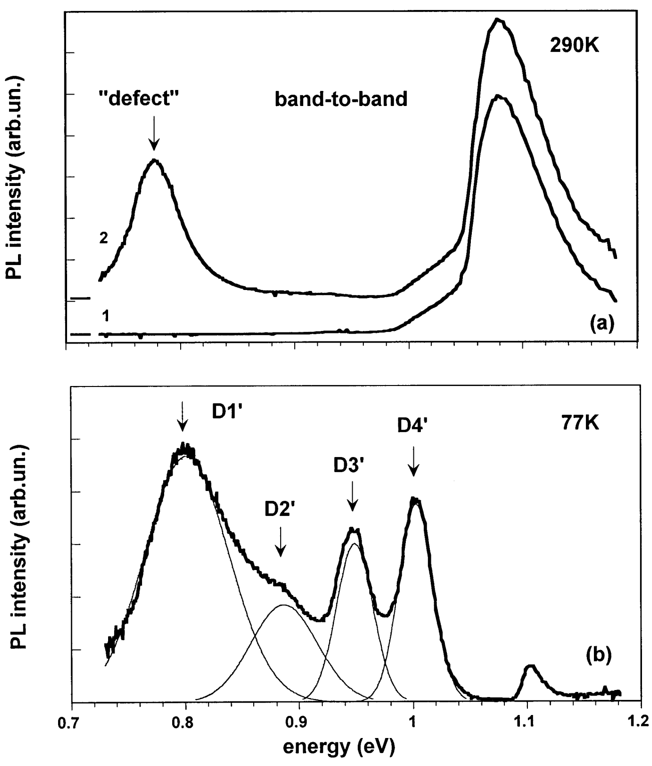

Fig. 1. (a) Room temperature PL spectrum measured in high lifetime region (1) and low lifetime region (2) of mc-Si wafer. (b) PL spectrum at 77 K and de-convolution on four individual sub bands. D1′ and D2′ lines correspond to 'defect' PL band at room temperature.

3. Results

Photoluminescence (PL) spectrum at room temperature is generally composed of two broad bands shown in Fig. 1a: (i) band-to-band emission with $h\nu_{max} = 1.09$ eV, and (ii) 'defect' band with maximum at about 0.78 eV which changes slightly across the wafer. Hereafter we assign the 'defect' band as the 0.8 eV band.

A room-temperature PL mapping was performed for both luminescence bands. First, we measured the band-to-band PL intensity (I_{bb}) in a scanning mode and compared this to a mapping of the effective minority carrier lifetime (τ_{eff}). In Fig. 2a and b, we presented a distribution of both values measured independently at the same wafer with equal steps. It is obvious, that the low-lifetime regions of the wafer (dark contrast) correspond to a noticeably reduced I_{bb} intensity and the opposite, high lifetime areas (white contrast) match to the increased band-to-band PL intensity. To illustrate this statement, one of the 'bad regions' is framed. This observation is quantified in Fig. 3 as a point-by-point plot of I_{bb} versus τ_{eff} for 1680-points map collected from a 5 × 5 cm mc-Si wafer (other sample). Notice a wide range of values in Fig. 3 spanning as much as one order of PL intensity and lifetime across the wafer. This is a consequence of a strong inhomogeneity of the starting mc-Si, which justify the necessity of developing scanning diagnostic techniques.

Based on data in Fig. 2a and b, and Fig. 3, it may be concluded that band-to-band PL intensity positively correlates to a distribution of the minority carrier lifetime in mc-Si. We notice that previously this was demonstrated in solar-grade bulk polycrystalline Si wafers grown by Edge-defined Film-fed Growth technology [1]. In a simple approximation one can assume that non-radiative centers are a dominant recombination channel in mc-Si at room temperature. The following relation is valid in this case:

$$I_{bb} \sim P_r/(P_r + P_{nr}) \sim \tau_n, \qquad (1)$$

where P_r and P_{nr} are the rates of radiative and non-radiative recombination, τ_n is a minority carrier lifetime. This relation is illustrated in Fig. 3.

We further observed that regions of mc-Si wafers possessing low lifetime values exhibit at room temperature an additional broad 'defect' band (I_{def}), with the maximum at about 0.8 eV (Fig. 1a, curve 2). It is important to note that in areas with high lifetime we were unable to detect the 0.8 eV PL band. A typical PL

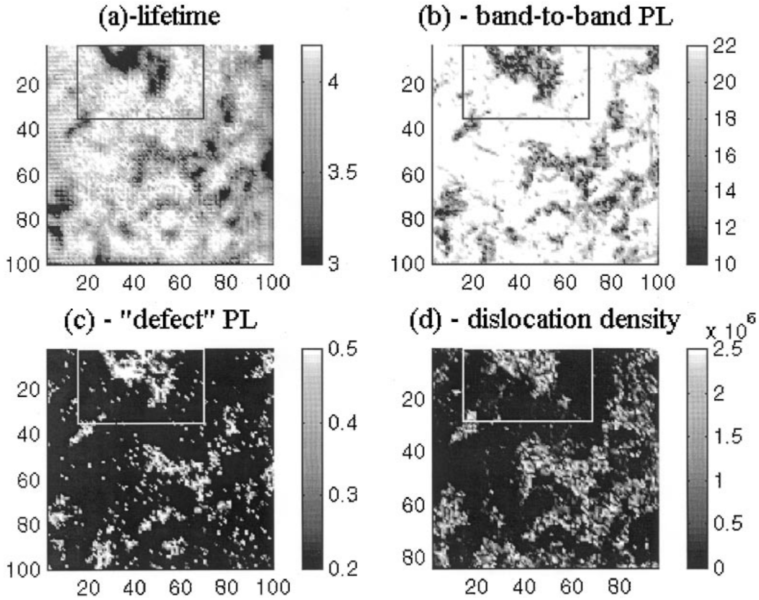

Fig. 2. (a) Minority carrier lifetime mapping with laser-microwave reflection, (b) band-to-band PL intensity (290 K), (c) 'defect' PL intensity (290 K), (d) dislocation density measured by EPD technique.

spectrum in a 'good region' of mc-Si is presented in Fig. 1 (curve 1). It was found previously that this band is observed in bare and processed polycrystalline EFG Si wafers and persists also in final solar cells [1]. Using PL mapping technique it was obvious that the 0.8 eV band is strongly localized in 'bad regions' showing a reverse contrast to lifetime and band-to-band PL intensity (Fig. 2c). This is clearly observed in the framed area corresponding to one of the 'bad regions' of the wafer. Concurrently with lifetime and PL mapping we performed at the same mc-Si wafer measurements of the dislocation density using EPD technique. The data presented in Fig. 2d document a positive correlation in distribution of the dislocation density with the 'defect' PL band. Specifically, the 0.8 eV PL band is observed in areas with dislocation density ranged $1-8\times 10^6$ cm^{-2}. We may conclude at this point that the 'defect' PL band is originating in areas with enhanced recombination activity and increased dislocation density.

To assess a possible origin of the 'defect' luminescence, we measured PL spectra at low temperatures down to 4.2 K and compared the areas with different recombination activity. The PL spectrum at 77 K of a 'bad region' in mc-Si wafer is depicted in Fig. 1b (thick line). The band-to-band luminescence is shifted to 1.1 eV due to temperature increasing of silicon band gap. Besides, the rich spectral features are now observed at energies below 1.05 eV. Two well-resolved bands have maximum at 0.95 and 1.00 eV correspondingly. At lower energies, the PL spectrum shows the maximum at 0.80 eV with barely resolved extra band as a shoulder. By increasing temperature up to 290 K we proved that the maximum at 0.8 eV is shifted to lower energies and traceable to the previously described 'defect' PL band (see Fig. 1a, curve 2). The PL spectroscopy was extended down to 4.2 K. At this temperature band-to-band emission is substituted with sharp excitonic lines dominated by the TO-phonon replica of the boron bound exciton at 1.093 eV. Aside from the total increase in PL intensity between 77 and 4.2 K, essentially no qualitative changes were observed in the PL spectrum below 1.05 eV. For this reason we limited our analyses with 77 K PL spectroscopy.

We performed a numeric deconvolution of the 77 K PL spectrum in the range of 0.72–1.05 eV, and found that it can be satisfactory decomposed by four individ-

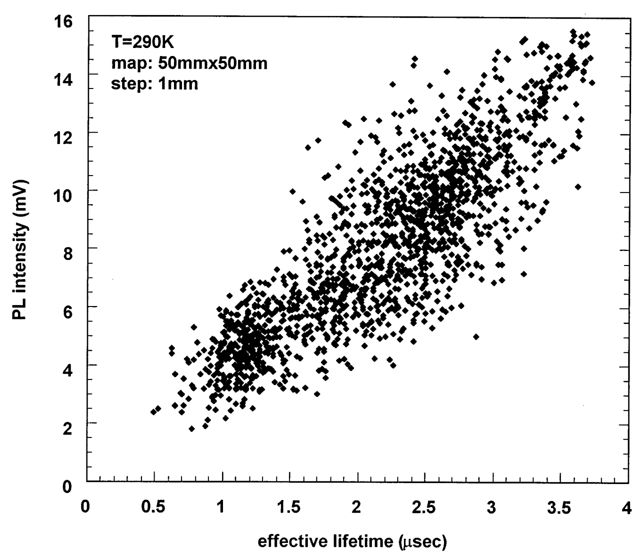

Fig. 3. Band-to-band PL intensity positively correlates to minority carrier lifetime (1680 points, 5 × 5 cm map-size).

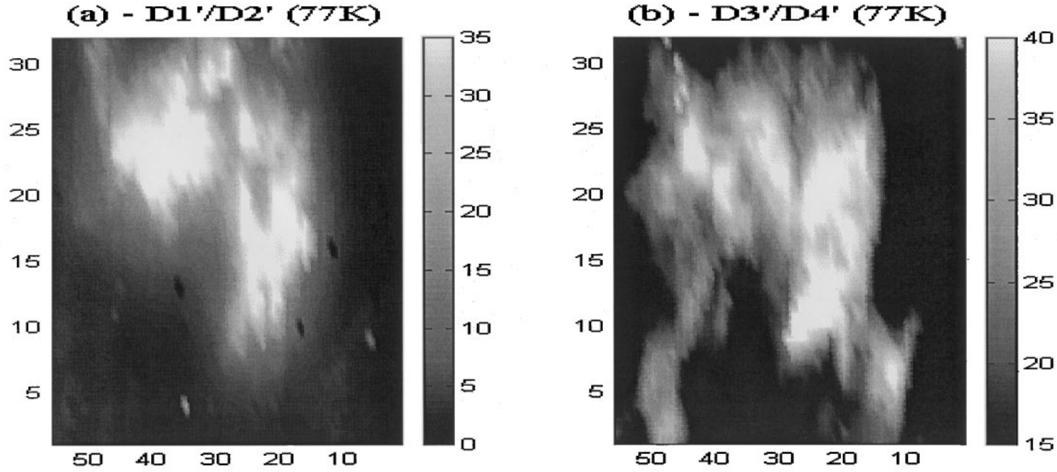

Fig. 4. PL mapping at 77K of the 'bad region' in mc-Si wafer (framed part in Fig. 2a) corresponding to D1′/D2′ band (a) and D3′/D4′ band (b).

ual Gaussian bands depicted by thin lines in Fig. 1b. It is remarkable that a set of four PL lines, known as D1 to D4, with very close energies (see Table 1) was previously observed and studied in detail in plastically deformed Cz–Si and attributed to the dislocation network [2,3]. It is worth noting that the range of dislocation density measured by EPD technique in 'bad regions' of mc-Si, $1-8\times10^{6}$ cm^{-2}, is close to that in plastically deformed Si exhibiting dislocation D-lines [2,3]. Due to this similarity, we assigned the individual bands in mc-Si as D1′–D4′ in the same sequence as dislocation D1–D4 lines. To challenge the dislocation origin of the D′-lines we measured the PL spectrum at 77 K under identical excitation in Cz–Si wafer with dislocations introduced by a laser annealing technique [4]. Four dislocation lines D1–D4 were clearly observed with maximum positions close to D′ bands (the entire set of D-lines was shifted by ≈ 10 meV presumably due to a strain field).

It is important to note that a half-width of the D3′/D4′ lines in mc-Si (≈ 30 meV) is close to the half-width of the D3/D4 in laser annealed Cz–Si. On the contrary, the D1′ and D2′ lines in mc-Si have an enlarged half-width by a factor of 2.5 compared to D1 and D2 lines in Cz–Si. Summarizing, a principal difference between dislocation D′-lines in mc-Si versus D-lines in Cz–Si is a substantial broadening (60–70 meV at 77K) of the D1′/D2′ lines, which accompanied by a different T-quenching of the D1′-line tracing to the intense room-temperature 'defect' luminescence. Therefore, the low-temperature PL spectroscopy additionally confirmed a linkage of the 'defect' luminescence in mc-Si to dislocations.

To accomplish a low-temperature PL study in mc-Si, we performed PL mapping at 77K of the D1′ band and comparing this with the D3′/D4′ luminescence measured in the area of high dislocation density. This area is framed in Fig. 2. An obvious correlation is observed in a way that high D1′/D2′ band intensity is observed in regions with enhanced D3′/D4′ lines. However, some areas of D3′/D4′ bands do not correspond to D1′/D2′. This is consistent with the model of the two sets of D-lines in plastically deformed Si suggesting that D1/D2 and D3/D4 belong to different entities [3].

4. Discussion

It is recognized that recombination-active dislocations in solar-grade mc-Si are a limiting factor to high efficiency solar cells. In this regard, presented experimental data of the room-temperature PL mapping are consistent with the dislocation origin of 'bad regions' in mc-Si wafers. Further, we can suggest that the 'defect' PL band in these regions originates from D1/D2 bands well known in plastically deformed Cz–Si wafers. A unique feature of these PL bands in mc-Si is that they are observed as a broad PL band retaining at room temperature opposite to the fact of a fast D1/D2 quenching in Cz–Si [3]. This difference can be addressed to (i) a strain field, which modifies recombination parameters of relevant centers, or/and (ii) interaction of dislocations with contamination precipi-

Table 1
Energy positions of dislocation D-lines in Cz–Si and D′ bands in mc-Si

Cz–Si [2]	D1	D2	D3	D4
	0.812	0.875	0.934	1.000
mc-Si	D1′	D2′	D3′	D4′
	0.80	0.89	0.95	1.00

tates. Specifically, it was observed that oxygen precipitates in Cz–Si influence a spectral position, half-width and intensity of the D1 line presumably due to a relaxation of the dislocation strain field [5]. This is consistent with the room temperature PL study of the 0.77 eV band attributed to oxygen precipitates in thermally treated Cz–Si [6]. Grain boundaries and dislocations in mc-Si are sinks for doping impurities and contamination including oxygen. Specifically, it was observed that the oxygen-enriched grain boundaries differ from oxygen deficient ones in terms of H-passivation [7]. Together these data imply that conventional hydrogenation employed to passivate recombination centers during solar cell processing may not be sufficient to eliminate the detrimental effect on carrier lifetime of oxygen precipitates at grain boundaries and dislocations.

In conclusion, scanning room temperature PL was applied to solar-grade mc-Si providing a deeper insight and advanced diagnostics of the 'bad regions' in solar cells. Band-to-band PL intensity is distributed similar to minority carrier lifetime and offers a reliable feedback to the bulk carrier recombination. A new advance to the scanning PL method is a mapping of the 'defect' band. In wafer regions with low lifetime values we observed a strong deep luminescence with the maximum at about 0.8 eV attributed to dislocation D1/D2 lines in silicon. PL mapping of this band can quantitatively assess recombination quality of solar-grade material at various steps of cell preparation. In fact, a ratio of the 'defect' PL intensity to the band-to-band PL intensity at room temperature is independent of other recombination channels and its mapping represents a convenient parameter for material or solar cell characterization. We can postulate that improved passivation of the 'defect' dislocation centers (e.g. an additional hydrogenation) may be a passage way to high-efficiency mc-Si solar cells.

Acknowledgements

We would like to thank Joerg Weber for critical comments. This work was supported by NREL grant XD-2-11004-5.

References

[1] Y. Koshka, S. Ostapenko, I. Tarasov, C. McHugo, J.P. Kalejs, Appl. Phys. Lett. 1555 (1999) 74.
[2] N.A. Drozdov, A.A. Patrin, V.D. Tkachev, JETP Lett. 598 (1976) 23.
[3] R. Sauer, J. Weber, J. Stolz, E.R. Weber, K.-H. Kusters, H. Alexander, Appl. Phys. 1 (1985) A36.
[4] W. Staiger, G. Pfeiffer, K. Weronek, A. Hopner, J. Weber, Mater. Sci. Forum 1571 (1994) 83–87.
[5] M. Bugajski, M. Goorsky, J. Lagowski, Electron. Technol. 85 (1991) 24.
[6] M. Tajima, M. Tokita, M. Warashina, Mater. Sci. Forum 1749 (1995) 196–201.
[7] E. Katz, M. Koltun, L. Polyak, Sol. State Phenom. 479 (1996) 51–52.